p47phox-Dependent NADPH Oxidase Regulates Flow-Induced Vascular Remodeling

Yves Castier, Ralf P. Brandes, Guy Leseche, Alain Tedgui, Stéphanie Lehoux

Abstract—Chronic alterations in blood flow elicit an adaptive response that tends to normalize shear stress, involving nitric oxide (NO) and matrix metalloproteinases (MMPs). To evaluate the role of NADPH oxidase in this process, we developed a new model of mouse arteriovenous fistula (AVF) connecting the right common carotid artery (RCCA) with the jugular vein, which does not affect blood pressure. Mice deficient for gp91phox and p47phox subunits of NADPH and wild-type controls were used. AVF greatly increased RCCA blood flow (0.78±0.12 to 4.71±0.78 mL/min; $P<0.01$), producing an abrupt rise in shear stress (35±1 to 261±17 dynes/cm^2; $P<0.01$) within 24 hours. RCCA diameter (460±14 μm) gradually enlarged 1 and 3 weeks after AVF (534±14 μm and 627±19 μm; $P<0.01$), reducing shear stress (173±13 and 106±10 dynes/cm^2, respectively). In gp91phox$^{-/-}$ mice, changes in RCCA caliber and shear stress matched controls. However, p47phox$^{-/-}$ mouse RCCAs enlarged only marginally, such that shear stress remained high (199±8 dynes/cm^2 at 3 weeks). Likewise, remodeling was minimal in endothelial NO synthase (eNOS)$^{-/-}$ mice. In both control and gp91phox$^{-/-}$ animals, reactive oxygen species (ROS) production and MMP induction was enhanced by AVF, whereas in p47phox$^{-/-}$ and eNOS$^{-/-}$ mice such response was negligible. Similarly, nitrotyrosine staining, indicating peroxynitrite formation, was more pronounced in control and gp91phox$^{-/-}$ mice than in p47phox$^{-/-}$ and eNOS$^{-/-}$ mice. Hence, shear stress induces vascular NADPH oxidase comprising p47phox but not gp91phox. Generated ROS interact with NO to produce peroxynitrite, which in turn activates MMPs, facilitating vessel remodeling. Our study provides the first evidence that ROS play a fundamental role in flow-induced vascular enlargement. (***Circ Res*****. 2005;97:533-540.)**

Key Words: extracellular matrix ■ metalloproteinases ■ reactive oxygen species ■ shear stress

Changes in blood flow drive both acute and long-term compensatory responses in the vascular wall that tend to normalize wall shear stress. In the case of persistent increases in flow, adaptive remodeling of the vessel involves the reorganization of cellular and extracellular components. This is best exemplified in models of arteriovenous fistula (AVF), where steep increases in flow result in extensive arterial enlargement through restructuring of the extracellular matrix and modulation of vascular cell synthetic capacity.[1]

One of the striking characteristics of the arterial wall proximal to an AVF is extensive tearing and fragmentation of the internal elastic lamina (IEL)[2,3] which augments arterial distensibility, leading to enhanced vessel diameter. Matrix metalloproteinases (MMPs) are likely instigators of IEL degradation in the vessel wall. MMP-2 and MMP-9 are upregulated shortly after AVF construction, and heightened activity of these enzymes persists until shear stress is normalized.[4,5] Furthermore, several studies have reported that MMP inhibition diminishes flow-mediated arterial enlargement in rat[4,6] and rabbit[5] AVF models, and prevents elastin degradation associated with AVF-induced arterial enlargement.[5]

MMPs are secreted as inactive zymogens (pro-MMPs) that require cleavage to become activated. Previous studies have highlighted a role for nitric oxide (NO) as an important regulator of MMP induction in flow-loaded vessels. In arteries exposed to chronic increases in blood flow, production of NO is enhanced[7] and endothelial nitric oxide synthase (eNOS) expression correlates with increased shear rate and arterial enlargement.[8] In addition, blockade of eNOS with N^G-nitro-L-arginine methyl ester (L-NAME) reduces MMP activation[5] and restricts artery enlargement upstream of an AVF.[3,9] On the other hand, several studies indicate that reactive oxygen species (ROS) are involved in MMP activation.[10,11] Thus it is likely that peroxynitrite, which results from simultaneous production of NO and superoxide anions, rather than NO itself, activates MMPs. Indeed, nitrotyrosine staining, indicative of the presence of peroxynitrite, is detectable in endothelial cells and throughout the media of flow-loaded carotid arteries of untreated rabbits but not in L-NAME treated animals.[5]

However, whereas the contribution of NO in flow-induced vascular remodeling has been well established by our group[3,5] and others,[9] the role of ROS in this context has not yet been

Original received March 24, 2005; revision received July 11, 2005; accepted August 4, 2005.

From INSERM Centre de Recherche Cardiovasculaire Lariboisière (Y.C., A.T., S.L.), Paris, France; Service de Chirurgie Vasculaire et Thoracique (Y.C., G.L.), Hôpital Beaujon, Clichy, France; and Institut für Kardiovaskuläre Physiologie (R.P.B.), Universität Frankfurt, Germany.

Correspondence to Dr Stephanie Lehoux, INSERM CRC Lariboisière, 41, Bd de la Chapelle, 75010 Paris, France. E-mail lehoux@larib.inserm.fr

Circulation Research **is available at http://circres.ahajournals.org** **DOI: 10.1161/01.RES.0000181759.63239.21**

defined. Moreover, it is not clear whether NADPH oxidase, one of the many enzymes able to generate ROS in the vasculature, contributes to this process. This study was therefore undertaken to evaluate the contribution of ROS, and the different NADPH oxidases, to the remodeling response observed in flow-loaded arteries. We used a new model of mouse carotid artery-jugular vein AVF, that allowed us to uncover the role of NADPH oxidase subunits in ROS generation using gp91phox- and p47phox-deficient mice. The necessary contribution of eNOS to this process was confirmed using eNOS$^{-/-}$ mice.

Materials and Methods

Adult male mice weighing 25 to 35 g (Charles River, France) were operated aseptically under general anesthesia, using a microscope. Animals were anesthetized using ketamine (0.2 mg/g i.p.) and xylazine (0.02 mg/g i.p.) and kept warm until complete awakening under a heating lamp. Each mouse received a bolus of heparin (1 U/g i.v.) at the onset of the operation. A transversal cervical incision was made, and the right jugular vein and common carotid artery (RCCA) were dissected free. Flow through the vein was interrupted by means of microvascular clamps, and the RCCA was clamped proximally and ligated distally. The RCCA was transected just proximal to the carotid bifurcation, and an end-to-side anastomosis was performed between vein and artery by making 6 interrupted 11-0 nylon sutures (Ethicon) under 3× magnification. The operative field was irrigated with a saline solution containing 100 U/mL heparin. Flow was then reestablished through the fistula by releasing the clamps. The incisions were closed with 6-0 vicryl, and the animals were allowed to recover. Operative time averaged 80 minutes and surgical success rate (fistula patent at 3 weeks) was ≈80%. Experiments were performed in accordance with the European Community Standards on the Care and Use of Laboratory Animals and were approved by the local ethics committee.

A first group of C57Bl/6 mice was used to establish a time course for artery remodeling. Animals were euthanized 0, 1, 7, 14, and 21 days postoperatively. Later times were not investigated because mice developed stenosis at the site of anastomosis, and vessel patency was reduced in many animals as of 28 days. Furthermore, no data were collected from animals with compromised flow attributable to thrombotic obstruction or stenosis. Additional experiments were performed using age and weight-matched gp91phox$^{-/-}$, p47phox$^{-/-}$, and eNOS$^{-/-}$ mice on a C57Bl/6 background, euthanized 0, 7, and 21 days postoperatively. Arterial pressure and heart rate were measured by tail cuff plethysmography (Visitech) before and at different times after AVF creation. Animal weight gain was equivalent in sham and fistulated mice, indicative that AVF did not induced pertubations leading to edema.

Hemodynamic Measurements

At the time of euthanasia, mice were anesthetized as indicated above, and both carotid arteries were exposed, the left CCA serving as a nonoperated internal control. The arteries were photographed in situ, alongside a 460 μm-wide scale placed parallel to the vessel, using a camera (Logitech) attached to the surgical microscope (Nikon). Precise arterial diameters were measured with the help of image analysis software (Histolab).

Blood flow velocity was measured by using a 20 MHz pulsed Doppler system (Milar). The pen probe position was adjusted to obtain a 30° angle with the vessel axis. Blood flow was measured 5 mm upstream of the AVF in the RCCA and at the equivalent location in the left CCA. Velocities (V, cm/sec) were obtained from the measured Doppler frequency shifts and volume flow (Q) was calculated by multiplying the mean velocity by the cross-sectional area of the vessel lumen, using the formula $Q\ (cm^3/s) = \pi\ r^2\ V$, where r is the radius in cm. Wall shear stress was calculated using the Poiseuille formula $\tau = 4\ \mu\ Q / \pi\ r^3$. In this formula, μ is the viscosity of blood (taken to be 0.035 poise).

Histological Analysis

After hemodynamic measurements, animals were killed by a bolus injection of sodium pentobarbital (0.5 mg/kg i.v.). Blood was washed out of the vasculature by perfusion at 100 mm Hg with normal saline solution through a cannula inserted in the abdominal artery. Arterial segments were embedded vertically in Tissue-tek (Sakura), and serial 10 μm sections were cut. Dihydroethidine (Sigma, 2×10^{-6} mol/L) was topically applied to tissue sections incubated 30 minutes at 37°C to reveal the presence of ROS as red fluorescence (585 nm).[12] MMP-2 and MMP-9 were detected using primary rabbit polyclonal antibodies used at 1:50 (Santa Cruz). Staining with a rabbit polyclonal anti-nitrotyrosine antibody (Upstate, 20 μg/mL) was used as an indicator of peroxynitrite formation.[5] Immunostainings were developed with avidin-biotin horseradish peroxidase (Vectastain ABC kit, Vector Laboratories). For in situ zymography, vessel sections were incubated at 37°C during 5 hours with a fluorogenic gelatin substrate (DQ gelatin, Molecular Probes) dissolved to 25 mg/mL in zymography buffer (50 mmol/L Tris-HCl pH 7.4 and 15 mmol/L $CaCl_2$).[13] Proteolytic activity was detected as green fluorescence (530 nm). All sections are shown with the adventitia facing upwards and the luminal aspect facing downwards. Semi-quantitative analysis of oxy-ethidium and gelatinase fluorescence, as well as nitro-tyrosine staining, was done independently by two individuals using Histolab software.

Luminescence Assay

Vessel ROS levels were also quantified using L-012 as described recently.[14] Carotid arteries were lysed in 50 mmol/L Tris buffer (pH 7.5) containing protease inhibitors (Boehringer) and lysates centrifuged at 10 000g for 15 minutes at 4°C. Supernatants were then incubated with 100 μmol/L L-012 (Wako) and luminescence counted (Perkin Elmer Topcount NXT) during 5 s after a 10 minute interval allowing for the plates to become dark-adapted.

In-Gel Zymography

To verify the role of nitrotyrosine in high shear stress-induced MMPs, 1 week fistulated arteries and contralateral controls were incubated during 24 hours in culture medium with or without ebselen (25 μmol/L). Thereafter arteries were lysed in nondenaturing laemmli buffer and lysates centrifuged at 10 000 rpm during 15 minutes. Lysate supernatants and vessel incubation media were eletrophoresed in SDS-PAGE gels containing 0.1% gelatin. Gels were washed twice in 2.5% triton and incubated overnight in zymography buffer (described above).

Statistical Analysis

Results are expressed as mean±SEM. Data were analyzed by one-way (for comparison of control versus AVF) or two-way ANOVA (for analysis of effects of different mouse strains). When ANOVA analyses yielded significant results, comparisons were done using Bonferroni's test. Differences were considered statistically significant at a value of $P<0.05$.

Results

Characterization of a New AVF Model in the Mouse

Creation of a shunt between the RCCA and jugular vein produced an abrupt increase in arterial blood flow, reaching more than 6-fold from the onset, as calculated on day 1 (Figure 1). Flow in the carotid artery remained consistently high during the following 3 weeks. In parallel, shear stress peaked at 261±16 dynes/cm^2 in the first day, from 37±2 before AVF, but diminished thereafter, returning toward baseline levels as the weeks progressed. This coincided with a rise in the arterial diameter, driven by enhanced wall shear stress. Appropriately, the most acute change in diameter (22%) was seen within the first 7 days, when shear stress was

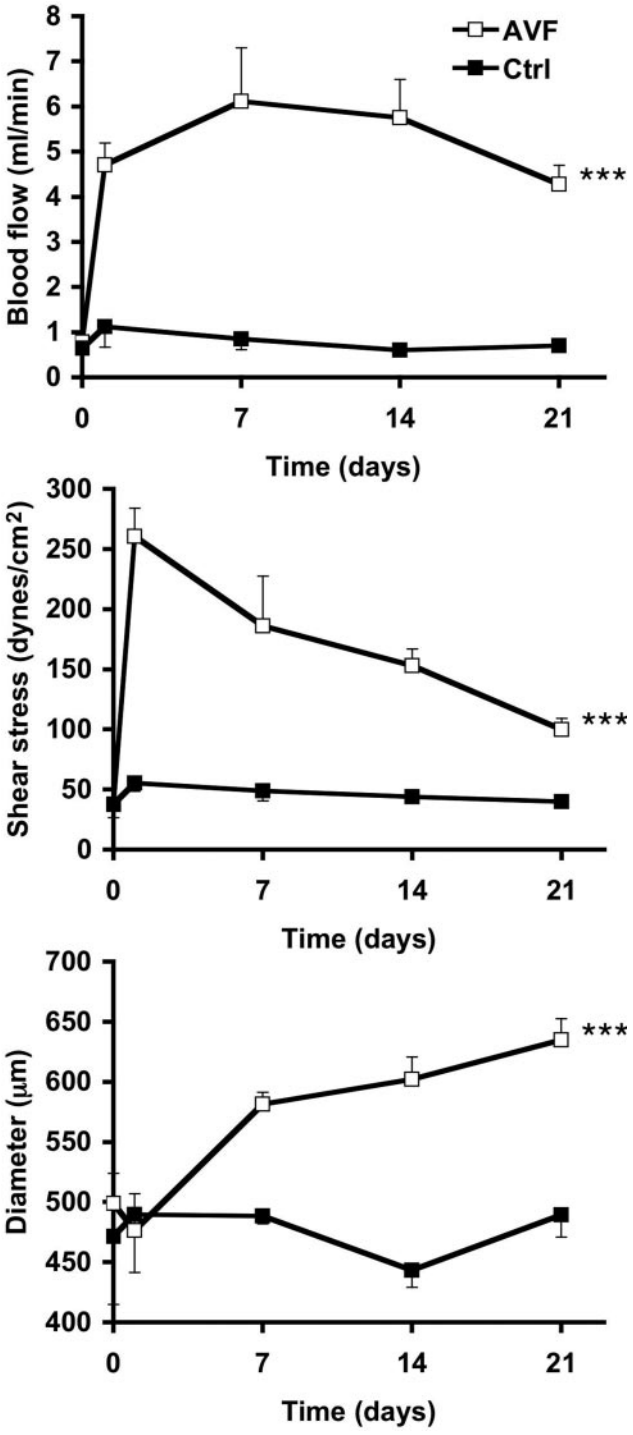

Figure 1. Characterization of the remodeling response in mouse carotid arteries before (day 0) and after AVF creation. Opening of the fistula induced an abrupt and persistent increase in carotid blood flow (upper). Shear stress in the carotid artery peaked immediately (day 1) after AVF creation, then decreased with time (middle). Carotid diameter, on the other hand, increased gradually over 3 weeks (lower). n=6 to 10, ***$P<0.001$ vs contralateral controls (Ctrl).

greatest (Figure 1). The RCCA enlarged more gradually (3% to 4% per week) during the subsequent weeks. Despite the marked increases in vessel diameter, no changes in artery thickness were observed (data not shown). No changes in

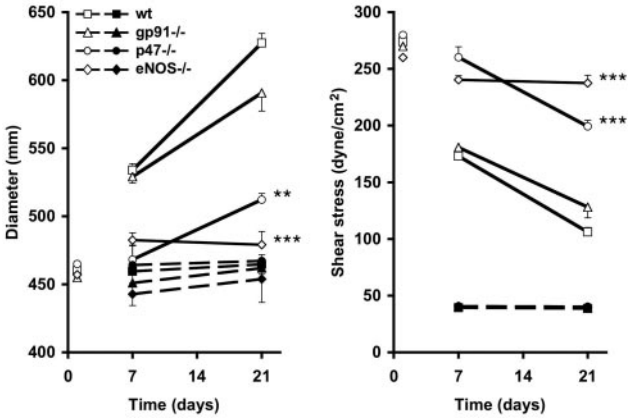

Figure 2. Remodeling is impaired in arteries from p47phox$^{-/-}$ and eNOS$^{-/-}$ mice. RCCA diameter (left) and shear stress (right) were assessed immediately after AVF opening, then 1 and 3 weeks thereafter (open symbols). Remodeling was equivalent in arteries of wild-type (wt) and gp91phox$^{-/-}$ mice; however, it was greatly reduced in p47phox$^{-/-}$ mice, which showed only a small increase in diameter at 3 weeks, and null in eNOS$^{-/-}$ mice. Appropriately, shear stress remained elevated in p47phox$^{-/-}$ and eNOS$^{-/-}$ mice compared with wild-type. Contralateral vessel diameter and shear stress did not vary at 1 and 3 weeks and did not differ between animals strains (closed symbols). n=4 to 10, **$P<0.01$ and ***$P<0.001$ vs wild-type RCCA.

blood flow or vessel diameter were observed in the contralateral artery.

Variations in RCCA diameter and shear stress could not be ascribed to altered blood pressure, as this parameter remained equivalent at all time points, before creation of the AVF (99±4 mm Hg) and after (100±7 mm Hg). Likewise, heart rate stayed stable before (651±8 bpm) and 1 (693±15) and 3 weeks (636±18) after surgery.

Vascular Remodeling in Vessels From gp91phox$^{-/-}$, p47phox$^{-/-}$, and eNOS$^{-/-}$ Mice

We postulated that production of ROS by NADPH oxidase could be a driving force behind vascular remodeling after AVF creation. This enzyme comprises several subunits including Nox proteins, of which gp91phox is an isoform known to be expressed in endothelial cells, and the ubiquitous p47phox. Hemodynamic measurements were therefore made in gp91phox$^{-/-}$ and p47phox$^{-/-}$ mice, and compared with data from wild-type and eNOS$^{-/-}$ mice. Baseline RCCA diameter and shear stress was equivalent in all animals before AVF creation (day 0), and these parameters did not vary in contralateral vessels throughout the experimental process (Figure 2). Flow levels in the fistulated arteries also increased equally in all mouse strains, reaching a mean of 4.43±0.02 mL/min after AVF creation compared with 0.64±0.02 mL/min before. Moreover, in wild-type and gp91phox$^{-/-}$ mice, flow-induced arterial enlargement was comparable both 1 and 3 weeks after AVF. Accordingly, shear stress diminished similarly with time in both groups. In contrast, no remodeling was observed in RCCAs of p47phox$^{-/-}$ mice at 1 week, but vessel diameter was significantly increased at 3 weeks ($P<0.01$ versus 1 week), suggesting that absence of ROS may have delayed the remodeling process rather than completely inhibiting it. Absence of remodeling was more marked

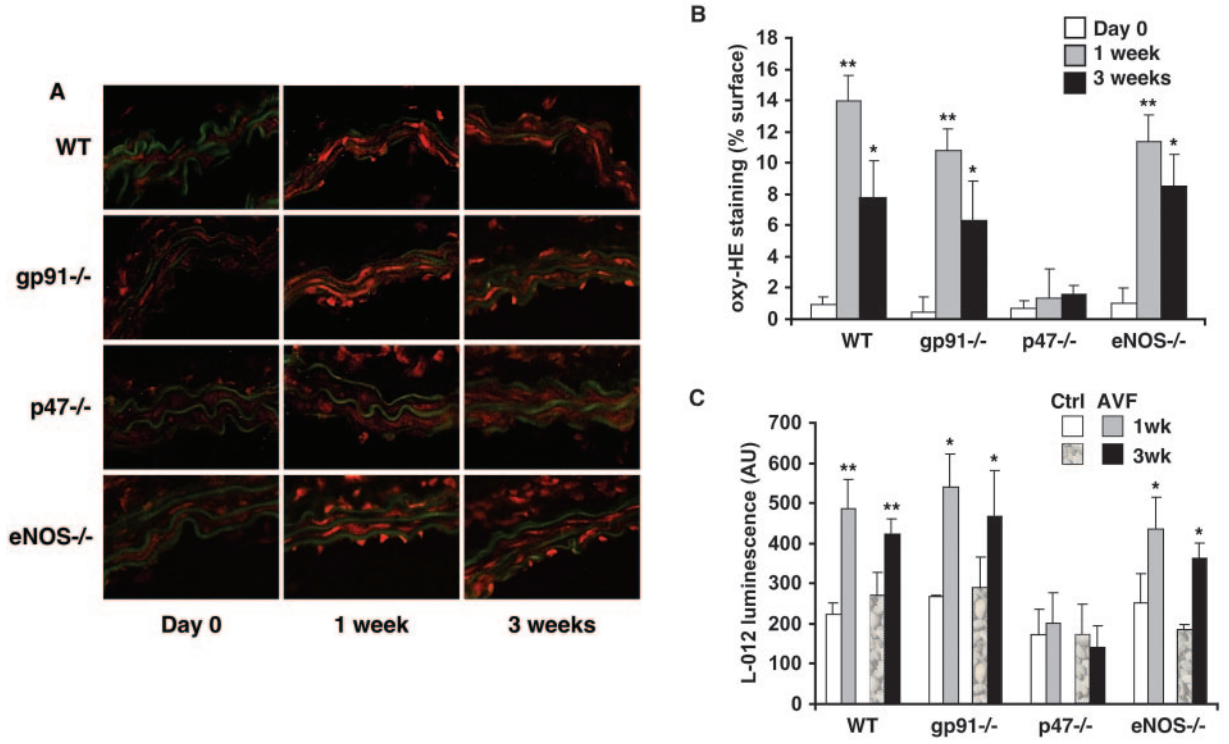

Figure 3. Flow-loaded vessels display enhanced ROS generation. A, Superoxide formation was evaluated by oxy-hydroethidine staining in RCCAs obtained before (day 0) and 1 and 3 weeks after AVF. Increased ROS production was visualized by amplified red fluorescence in the endothelium and throughout the vessel wall of wild-type, gp91phox$^{-/-}$ and eNOS$^{-/-}$ mice. In comparison, staining was much more moderate in arteries of p47phox$^{-/-}$ animals. Autofluorescent elastic laminae appear as green bands. B, Semiquantitative analysis of oxy-hydroethidine staining confirmed significant ROS production in flow-loaded arteries from wild-type, gp91phox$^{-/-}$, and eNOS$^{-/-}$ mice. n=4, *P<0.05 and **P<0.01 vs day 0. C, This was further substantiated by a luminescence assay of whole vessel lysates. n=3 to 6, *P<0.05 and **P<0.01 vs contralateral control (ctrl).

in eNOS$^{-/-}$ animals, where high shear stress completely failed to stimulate arterial enlargement.

NADPH Oxidase Is the Source of Shear Stress-Induced ROS

To verify that ROS were actually produced in flow-loaded vessels, carotid artery sections were incubated with dihydroethidine, which in the presence of superoxide anions is transformed to oxy-ethidium. In unoperated RCCAs from wild-type animals (day 0), low levels of ROS were detected. However, at 1-week post-AVF oxy-ethidium fluorescence was much more substantial, being significantly enhanced (P<0.01) throughout the vascular wall (Figure 3A and 3B). Superoxide levels remained elevated at the 3-week time point (P<0.05). In flow-loaded arteries of gp91phox$^{-/-}$ mice, ROS production was not hindered, whereas it was greatly reduced in p47phox$^{-/-}$ animals, both at 1 and 3 weeks after AVF creation. Absence of eNOS, on the other hand, did not interfere with ROS production in arteries under high shear stress.

These results were substantiated by L-012 luminescence, wherein ROS production in flow-loaded arteries was compared with that in contralateral vessels. In wild-type, gp91$^{-/-}$ and eNOS$^{-/-}$ animals, AVF construction was associated with a significant (P<0.05) increase in vascular ROS production, both at 1 and at 3 weeks (Figure 3C). In arteries from p47$^{-/-}$ mice, however, no increment in ROS production could be detected after AVF.

MMP Induction in the AVF

NADPH oxidase-dependent ROS generated in flow-loaded vessels could presumably react with NO to produce peroxynitrite, revealed by nitrotyrosine. Indeed, in congruence with ROS production, staining for nitrotyrosine was very marked in RCCAs of wild-type and gp91phox$^{-/-}$ mice, both at the 1 week time point (P<0.01) and at 3 weeks (P<0.05), whereas it appeared only weakly in arteries of p47phox$^{-/-}$ mice, only significantly so (P<0.05) at 1 week. (Figure 4 A and 4B). Nitrotyrosine staining was absent from flow-loaded RCCAs of eNOS$^{-/-}$ animals, indicating that locally generated NO contributed to peroxynitrite formation.

Positive nitrotyrosine staining turned out to be a good predictor of MMP activation in carotid arteries. As shown in Figure 5A and 5B, in situ gelatinolytic activity was enhanced in flow-loaded RCCAs of wild-type and gp91phox$^{-/-}$ mice, being greatest 1 week after AVF (P<0.001 and P<0.05, respectively), and remaining elevated at 3 weeks (P<0.01 and P<0.05, respectively). In comparison, neither p47phox$^{-/-}$ nor eNOS$^{-/-}$ mice-derived carotid arteries generated significant gelatinase activity when exposed to high shear stress. In added proof, gelatinase activity was assessed in 1-week flow-loaded and contralateral arteries from wild-type mice, incubated 24 hours in culture medium. In both

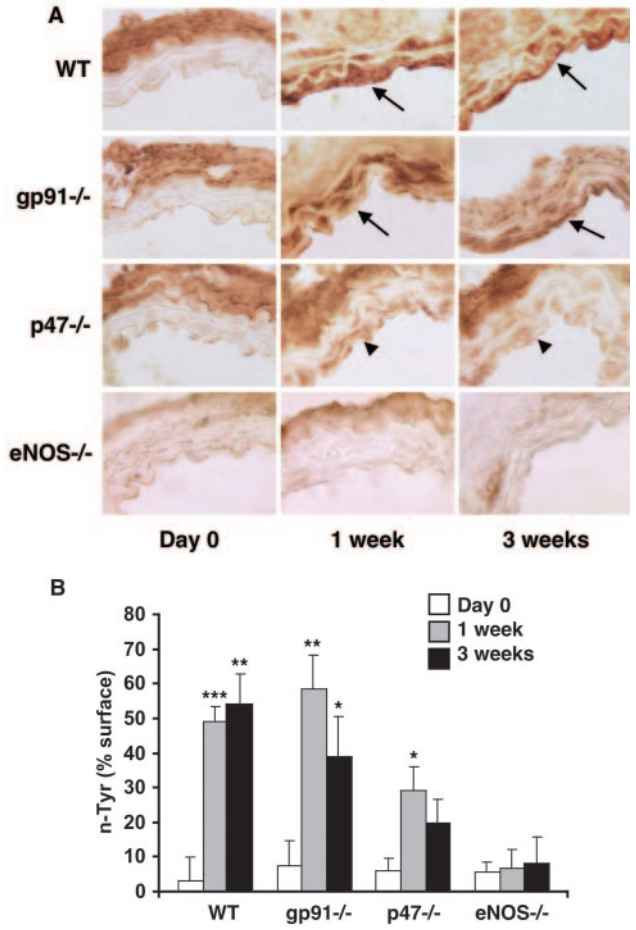

Figure 4. A, Peroxynitrite formation was strongly accentuated in fistulated arteries of wild-type and gp91phox$^{-/-}$ mice, as evidenced by positive nitrotyrosine staining (arrows) 1 and 3 weeks after AVF creation. However, production of peroxynitrite was quite low in arteries of p47phox$^{-/-}$ mice (arrowheads) and was completely absent in vessels of eNOS$^{-/-}$ animals. B, Semiquantitative analysis of peroxynitrite staining in the vessel wall. n=4, *P<0.05, **P<0.01, and ***P<0.01 vs day 0.

artery lysates and incubation media, high flow was associated with increased MMP2 and MMP9 levels, compared with contralateral controls (Figure 5C). After treatment with ebselen, to block peroxynitrite, MMP activity was reduced in whole vessels, and release of MMPs in the incubation media was abolished.

Interestingly, fluorescence was noticeably accentuated in the innermost vessel layer, indicative of high gelatinase activity in the endothelium (Figure 5A). This corresponded to the particularly strong endothelial staining for MMP-9, which was induced in flow-loaded vessels of wild-type, and gp91phox$^{-/-}$ animals (Figure 6). Absence of staining in p47phox$^{-/-}$ and eNOS$^{-/-}$ suggests that ROS and NO could participate not only in the activation of MMPs, but could also modulate their protein expression in conditions of high shear stress. In comparison, MMP-2 levels did not differ between arteries at normal or elevated flow levels, whatever the mouse strain used (data not shown). However, we know from previous AVF models[5] that induction of MMP-2 occurs early on, so it may have peaked and waned before the 1-week time point.

Discussion

The present study demonstrates that ROS production is enhanced in arteries exposed to chronic high flow and plays an active role in vascular remodeling. Moreover, we show that NADPH oxidase comprising the p47phox subunit is the major generator of shear stress-induced ROS in the vascular wall; gp91phox, in comparison, plays a negligible role in this process. Together with NO derived from eNOS activation, ROS produces peroxynitrite, which in all probability accounts for MMP activation and enlargement of flow-loaded vessels.

Changes in shear stress have previously been associated with an increase in ROS production. In coronary resistance arteries, increasing flow rate is associated with an enhanced H_2O_2 production, and scavenging the H_2O_2 with catalase impairs acute flow-induced dilatation.[15] However, thus far there has been little information regarding the source of ROS in vessels exposed to high shear or flow. It was recently proposed that H_2O_2 originating from mitochondrial respiration could account for flow-induced dilatation in human coronary arteries.[16] Enhanced ROS production in arteries exposed to acute shear was abolished by combined treatment with free radical scavengers superoxide dismutase and catalase, as well as the mitochondrial complex I and III inhibitors rotenone and myxothiazol, but was not affected by the NADPH oxidase inhibitor apocynin.[16] Nevertheless, others have pointed out a role for NADPH oxidase as a possible generator of ROS in endothelial cells stimulated by shear stress. Silacci et al[17] showed that 24 hours of pulsatile shear stress with a low mean shear stress (6±3 dynes/cm^2) enhanced superoxide production and upregulated p22phox expression in endothelial cells. Likewise, the mRNA expression of both gp91phox and Nox4 was upregulated in endothelial cells exposed during 4 to 8 hours to oscillatory flow, concomitant with a rise in detected ROS that was blocked by depleting cellular NADPH levels.[18] However, pulsatile flow with a high mean shear stress (25±3 dynes/cm^2) did not stimulate ROS in cultured endothelial cells,[18] corroborating a previous finding that laminar shear stress induces a transitory activation of NADPH oxidase, whereas the effect of oscillatory shear is more prolonged.[19] Here we show unequivocally that a chronic increase in blood flow activates the vascular production of ROS that persists as long as the flow-loaded vessels perceive abnormally high shear stress. This differs from in vitro experiments where laminar or pulsatile mean shear stress is close to physiological values, and transient superoxide generation occurs because cells react to a change in shear rate. Indeed, in our contralateral vessels, shear stress levels were normal and ROS production remained low.

The current report is the first to demonstrate that NADPH oxidase is directly implicated in ROS production in vessels exposed to elevated shear stress, and that ROS participate in flow-induced vascular remodeling. NADPH oxidase is in fact composed of several phox (*ph*agocytic respiratory burst *ox*idase) elements that assemble on activation. Seven homologues of the catalytic subunit exist, of which Nox1, Nox2 (gp91phox), Nox4 and Nox5 are found in the endothelium.[20,21] Vascular wall distribution of NADPH oxidase is not homogenous: gp91phox is involved in the oxidase activity of the endothelium and the adventitia only,[22] whereas in SMC,

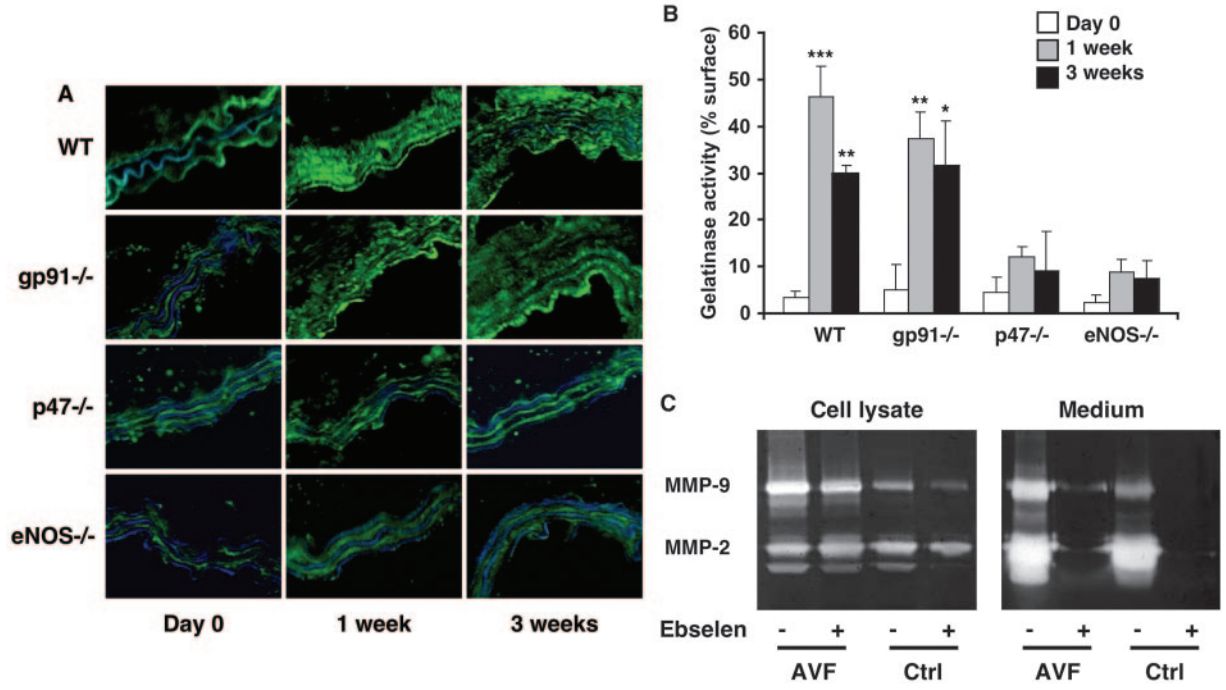

Figure 5. In situ gelatinase assay reveals high MMP activity in the endothelium and medial portions of flow-loaded arteries. A, Fluorescence was enhanced in vessels of wild-type and gp91phox$^{-/-}$ mice 1 and 3 weeks after AVF but showed little change in intensity in arteries of p47phox$^{-/-}$ and eNOS$^{-/-}$ mice. Autofluorescent elastic laminae appear as blue bands. B, Semiquantitative analysis of gelatinase fluorescence in the vessel wall. n=4, *P<0.05, **P<0.01, and ***P<0.01 vs day 0. C, Gelatin zymography showing MMP-2 and MMP-9 activity in cell lysates (left) and media (right) of 1-week fistulated or contralateral arteries placed 24 hour in culture medium, with or without ebselen. Representative of 3 separate experiments.

gp91phox is mostly replaced by Nox1.[23] However, the oxidase in all layers of the vascular wall requires the organizing subunit p47phox.[24,25] Our observation that ROS production and vascular remodeling in flow-loaded arteries of gp91phox$^{-/-}$ mice was equivalent to that of wild-type animals strongly suggests that another Nox subunit is involved in these processes. Although Nox4 is expressed in greater abundance than any other Nox homologue in vascular cells,[23,26] it is thought that Nox4 sustains a constitutive low level ROS formation in resting cells.[27,28] Most importantly, Nox4 does not require the cytosolic NADPH oxidase organizer p47phox (or its homologue Noxo1) for ROS production.[29] The data of the present study clearly indicate that p47phox is involved in ROS production in flow-loaded arteries, suggesting that Nox4 may not be the source of ROS. The activity of the Nox1 homologue, in contrast, is dependent on an organizing subunit such as p47phox,[30] and Nox1 mediated signaling in endothelial cells exposed to oscillatory shear stress is prevented by downregulation of p47phox.[31] Therefore, Nox1 may very well be the Nox isoform acting in conjunction with p47phox to regulate flow-induced vascular remodeling.

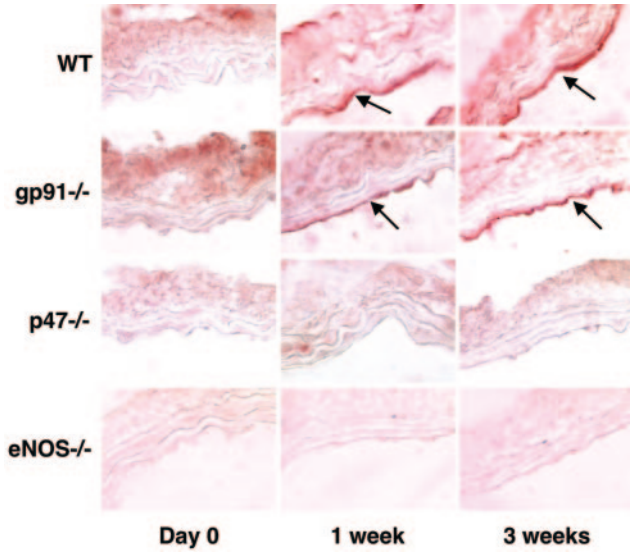

Figure 6. High flow is associated with upregulation of MMP-9 in RCCAs of wild-type and gp91phox$^{-/-}$ mice. One and 3 weeks after AVF creation, MMP-9 staining was enhanced in the innermost artery layers (arrows), compared with day 0. In vessels of p47phox$^{-/-}$ and eNOS$^{-/-}$ mice, however, no MMP-9 was detectable at any time point.

It should be pointed out that ROS production was not completely abolished in flow-loaded vessels of p47phox$^{-/-}$ mice, probably an indication of mitochondrial free radical production.[16] Nevertheless, such minimal ROS levels were clearly not sufficient to support flow-induced arterial enlargement, at least in the early phase, even if they did allow for a small increment in peroxynitrite generation and a marginal increase in MMP activity in the media. We did observe a significant increase in vessel diameter in flow-loaded vessels from p47$^{-/-}$ mice at the 3-week time point, indicating that at length some remodeling could occur, probably attributable to the cumulative effect of the low level MMPs.

An observation that stands out from our data is that MMP-9 was induced in the endothelium of flow-loaded

arteries of wild-type and gp91phox$^{-/-}$ mice, but not at all in p47phox$^{-/-}$ mice, nor in eNOS$^{-/-}$ animals. This suggests that NADPH oxidase is involved in regulating MMP-9 expression by shear stress. Interestingly, in smooth muscle cells exposed to cyclic stretch, MMP-2 upregulation also depends on the presence of p47phox,[10] indicating that NADPH oxidase-derived ROS may bridge the gap between mechanical strain and MMP production in different types of vascular cells. Similarly, though the role of NO in regulating MMP expression is ambivalent,[32] the current study establishes that MMP-9 induction in the setting of enhanced shear stress requires eNOS. It follows that MMP activation was particularly amplified in the endothelium of flow-loaded arteries, in parallel with MMP-9 expression, and this upregulation correlated with substantial vascular remodeling. Hence, endothelial MMP induction and activation appears to be determinant in promoting flow-induced vascular remodeling, probably because it modulates rapid degradation of the internal elastic lamina, an essential step in AVF enlargement.[2,3] Fittingly, deendothelialized segments of flow-loaded rat and rabbit common carotid arteries fail to dilate and remodel.[3,33] It is likely that at length, persistent vessel dilation attributable to elevated shear stress translated to a stretch stimulus for the underlying smooth muscle cells, accounting for the observed production of MMPs throughout the vessel wall rather than in endothelial cells alone. However, we have previously shown that MMPs are activated soon after AVF creation,[3] at a time when vessel caliber has not dramatically changed, clearly indicating that the primary trigger for MMP activation is shear rather than stretch.

Perhaps one limitation of the mouse carotid fistula model is that remodeling was not complete at 3 weeks, because shear stress had not yet returned to physiological baseline values.[34] This might appear surprising, given that fistulated rabbit carotid arteries remodeled entirely 15 days after AVF.[5] However, the adaptive response to great stresses appears to require a longer period of time, as shown using the monkey iliac artery, where restoring shear stress to a baseline value after a 10-fold increase in flow required 6 months.[35] Nonetheless, mouse carotid enlargement did allow for a compensatory reduction shear stress from more than 7-fold of controls on fistula opening to less than 2-fold at 3 weeks, and would probably have progressed until shear stress returned to normal levels had fistula permeability not become compromised beyond that time point.

In summary, this is the first study using a mouse carotid fistula model to investigate the molecular mechanisms of shear stress-induced vascular remodeling. Observations made in p47phox$^{-/-}$ mice and eNOS$^{-/-}$ mice provide direct evidence that endogenous ROS and NO modulate not only the activity of MMPs, but also their production, in arteries exposed to elevated blood flow. Staining for peroxynitrite, which was enhanced in fistulated vessels from wild-type mice but not p47phox- or eNOS-deficient animals, reinforces the premise that peroxynitrite is a major activator of MMPs in this setting. Combined with NO, NADPH oxidase-derived ROS therefore appear to play an extensive role in blood flow-induced vascular remodeling, and are probably key mediators of the long term structural adaptation to altered blood flow.

Acknowledgments

This work emanates from the European Vascular Genomics Network (http://www.evgn.org), a Network of Excellence supported by the European Community's sixth Framework Programme for Research Priority 1 "Life sciences, genomics and biotechnology for health" (Contract No. LSHM-CT-2003-503254), and the German Research Foundation (DFG BR 1839/2-1).

References

1. Lehoux S, Tronc F, Tedgui A. Mechanisms of blood flow-induced vascular enlargement. *Biorheology*. 2002;39:319–324.
2. Greenhill NS, Stehbens WE. Scanning electron microscopic investigation of the afferent arteries of experimental femoral arteriovenous fistulae in rabbits. *Pathology*. 1987;19:22–27.
3. Tronc F, Wassef M, Esposito B, Henrion D, Glagov S, Tedgui A. Role of NO in flow-induced remodeling of the rabbit common carotid artery. *Arterioscler Thromb Vasc Biol*. 1996;16:1256–1262.
4. Karwowski JK, Markezich A, Whitson J, Abbruzzese TA, Zarins CK, Dalman RL. Dose-dependent limitation of arterial enlargement by the matrix metalloproteinase inhibitor RS-113,456. *J Surg Res*. 1999;87:122–129.
5. Tronc F, Mallat Z, Lehoux S, Wassef M, Esposito B, Tedgui A. Role of matrix metalloproteinases in blood flow-induced arterial enlargement. *Arterioscler Thromb Vasc Biol*. 2000;20:e120–e126.
6. Abbruzzese TA, Guzman RJ, Martin RL, Yee C, Zarins CK, Dalman RL. Matrix metalloproteinase inhibition limits arterial enlargements in a rodent arteriovenous fistula model. *Surgery*. 1998;124:328–334.
7. Miller VM, Burnett JCJ. Modulation of NO and endothelin by chronic increases in blood flow in canine femoral arteries. *Am J Physiol*. 1992;263:H103–H108.
8. Tuttle JL, Nachreiner RD, Bhuller AS, Condict KW, Connors BA, Herring BP, Dalsing MC, Unthank JL. Shear level influences resistance artery remodeling: wall dimensions, cell density, and eNOS expression. *Am J Physiol Heart Circ Physiol*. 2001;281:H1380–H1389.
9. Guzman RJ, Abe K, Zarins CK. Flow-induced arterial enlargement is inhibited by suppression of nitric oxide synthase activity in vivo. *Surgery*. 1997;122:273–279.
10. Grote K, Flach I, Luchtefeld M, Akin E, Holland SM, Drexler H, Schieffer B. Mechanical stretch enhances mRNA expression and proenzyme release of matrix metalloproteinase-2 (MMP-2) via NAD(P)H oxidase-derived reactive oxygen species. *Circ Res*. 2003;92:e80–e86.
11. Rajagopalan S, Meng XP, Ramasamy S, Harrison DG, Galis ZS. Reactive oxygen species produced by macrophage-derived foam cells regulate the activity of vascular matrix metalloproteinases in vitro. Implications for atherosclerotic plaque stability. *J Clin Invest*. 1996;98:2572–2579.
12. Lehoux S, Esposito B, Merval R, Loufrani L, Tedgui A. Pulsatile stretch-induced extracellular signal-regulated kinase 1/2 activation in organ culture of rabbit aorta involves reactive oxygen species. *Arterioscler Thromb Vasc Biol*. 2000;20:2366–2372.
13. Lehoux S, Lemarie CA, Esposito B, Lijnen HR, Tedgui A. Pressure-induced matrix metalloproteinase-9 contributes to early hypertensive remodeling. *Circulation*. 2004;109:1041–1047.
14. Daiber A, Oelze M, August M, Wendt M, Sydow K, Wieboldt H, Kleschyov AL, Munzel T. Detection of superoxide and peroxynitrite in model systems and mitochondria by the luminol analogue L-012. *Free Radic Res*. 2004;38:259–269.
15. Miura H, Bosnjak JJ, Ning G, Saito T, Miura M, Gutterman DD. Role for hydrogen peroxide in flow-induced dilation of human coronary arterioles. *Circ Res*. 2003;92:e31–e40.
16. Liu Y, Zhao H, Li H, Kalyanaraman B, Nicolosi AC, Gutterman DD. Mitochondrial sources of H_2O_2 generation play a key role in flow-mediated dilation in human coronary resistance arteries. *Circ Res*. 2003;93:573–580.
17. Silacci P, Desgeorges A, Mazzolai L, Chambaz C, Hayoz D. Flow pulsatility is a critical determinant of oxidative stress in endothelial cells. *Hypertension*. 2001;38:1162–1166.
18. Hwang J, Ing MH, Salazar A, Lassegue B, Griendling K, Navab M, Sevanian A, Hsiai TK. Pulsatile versus oscillatory shear stress regulates NADPH oxidase subunit expression: implication for native LDL oxidation. *Circ Res*. 2003;93:1225–1232.

19. De Keulenaer GW, Chappell DC, Ishizaka N, Nerem RM, Alexander RW, Griendling KK. Oscillatory and steady laminar shear stress differentially affect human endothelial redox state: role of a superoxide-producing NADH oxidase. *Circ Res*. 1998;82:1094–1101.
20. Brandes RP, Kreuzer J. Vascular NADPH oxidases: molecular mechanisms of activation. *Cardiovasc Res*. 2005;65:16–27.
21. Griendling KK. Novel NAD(P)H oxidases in the cardiovascular system. *Heart*. 2004;90:491–493.
22. Gorlach A, Brandes RP, Nguyen K, Amidi M, Dehghani F, Busse R. A gp91phox containing NADPH oxidase selectively expressed in endothelial cells is a major source of oxygen radical generation in the arterial wall. *Circ Res*. 2000;87:26–32.
23. Lassegue B, Sorescu D, Szocs K, Yin Q, Akers M, Zhang Y, Grant SL, Lambeth JD, Griendling KK. Novel gp91(phox) homologues in vascular smooth muscle cells : Nox1 mediates angiotensin II-induced superoxide formation and redox-sensitive signaling pathways. *Circ Res*. 2001;88:888–894.
24. Landmesser U, Cai H, Dikalov S, McCann L, Hwang J, Jo H, Holland SM, Harrison DG. Role of p47(phox) in vascular oxidative stress and hypertension caused by angiotensin II. *Hypertension*. 2002;40:511–515.
25. Brandes RP, Miller FJ, Beer S, Haendeler J, Hoffmann J, Ha T, Holland SM, Gorlach A, Busse R. The vascular NADPH oxidase subunit p47phox is involved in redox-mediated gene expression. *Free Radic Biol Med*. 2002;32:1116–1122.
26. Szocs K, Lassegue B, Sorescu D, Hilenski LL, Valppu L, Couse TL, Wilcox JN, Quinn MT, Lambeth JD, Griendling KK. Upregulation of Nox-based NAD(P)H oxidases in restenosis after carotid injury. *Arterioscler Thromb Vasc Biol*. 2002;22:21–27.
27. Ago T, Kitazono T, Ooboshi H, Iyama T, Han YH, Takada J, Wakisaka M, Ibayashi S, Utsumi H, Iida M. Nox4 as the major catalytic component of an endothelial NAD(P)H oxidase. *Circulation*. 2004;109:227–233.
28. Ellmark SH, Dusting GJ, Fui MN, Guzzo-Pernell N, Drummond GR. The contribution of Nox4 to NADPH oxidase activity in mouse vascular smooth muscle. *Cardiovasc Res*. 2005;65:495–504.
29. Ambasta RK, Kumar P, Griendling KK, Schmidt HH, Busse R, Brandes RP. Direct interaction of the novel Nox proteins with p22phox is required for the formation of a functionally active NADPH oxidase. *J Biol Chem*. 2004;279:45935–45941.
30. Banfi B, Clark RA, Steger K, Krause KH. Two novel proteins activate superoxide generation by the NADPH oxidase NOX1. *J Biol Chem*. 2003;278:3510–3513.
31. Sorescu GP, Song H, Tressel SL, Hwang J, Dikalov S, Smith DA, Boyd NL, Platt MO, Lassegue B, Griendling KK, Jo H. Bone morphogenic protein 4 produced in endothelial cells by oscillatory shear stress induces monocyte adhesion by stimulating reactive oxygen species production from a nox1-based NADPH oxidase. *Circ Res*. 2004;95:773–779.
32. Galis ZS, Khatri JJ. Matrix metalloproteinases in vascular remodeling and atherogenesis: the good, the bad, and the ugly. *Circ Res*. 2002;90:251–262.
33. Tohda K, Masuda H, Kawamura K, Shozawa T. Difference in dilatation between endothelium-preserved and -desquamated segments in the flow-loaded rat common carotid artery. *Arterioscler Thromb*. 1992;12:519–528.
34. Kamiya A, Togawa T. Adaptive regulation of wall shear stress to flow change in the canine carotid artery. *Am J Physiol*. 1980;239:H14–H21.
35. Zarins CK, Zatina MA, Giddens DP, Ku DN, Glagov S. Shear stress regulation of artery lumen diameter in experimental atherogenosis. *J Vasc Surg*. 1987;5:413–420.

Circulation Research
JOURNAL OF THE AMERICAN HEART ASSOCIATION

p47phox-Dependent NADPH Oxidase Regulates Flow-Induced Vascular Remodeling

Yves Castier, Ralf P. Brandes, Guy Leseche, Alain Tedgui and Stéphanie Lehoux

Circ Res. 2005;97:533-540; originally published online August 18, 2005;
doi: 10.1161/01.RES.0000181759.63239.21
Circulation Research is published by the American Heart Association, 7272 Greenville Avenue, Dallas, TX 75231

Print ISSN: 0009-7330. Online ISSN: 1524-4571